Available online at www.sciencedirect.com
ScienceDirect
Journal of Nuclear Materials 358 (2006) 209–216
journal of nuclear materials
www.elsevier.com/locate/jnucmat

Molecular dynamics simulation study of primary damage in UO_2 produced by cascade overlaps

L. Van Brutzel *, M. Rarivomanantsoa

Commissariat à l'Énergie Atomique, CEA/DEN-DTCD-SECM-LCLT, CEA-Marcoule B.P. 17171, Bagnols sur cèze cedex 30207, France

Received 5 April 2006; accepted 14 July 2006

Abstract

Molecular dynamics (MD) simulation is used to simulate the primary damage state due to α-self-irradiation in a UO_2 matrix. This study is carried out by simulating a set of 5 keV displacement cascades. Primary knock-on atom (PKA) direction and temperature are found not to influence the creation of point defects and point defects clustering. In the cascade overlap sequences the number of point defects created saturates as the dose increases. Large clusters of vacancies are observed toward the end of the overlap sequences. These clusters are stable within the time scale of the MD simulations. Interstitial clusters are found to be small and isolated.

PACS: 61.72.Ji; 61.803.Az; 61.80.Lj

1. Introduction

In storage or repository conditions, the uranium dioxide (UO_2) matrix undergoes structural damage due to self-irradiation. It has been shown that most of the energy provided by β- and γ-decays is dissipated via electronic excitations [1,2]. On the other hand, a 4 MeV α-particle produces both electronic excitations and ballistic shocks due to the recoil of a daughter nucleus. These ballistic shocks lead to numerous atomic displacements and significant structural damages. However, even at high energy irradiations no amorphisation has been observed [3–5]. The UO_2 matrix damage is mainly composed of local defects such as vacancies and interstitials. These defects can gather and cause further dislocations and stacking faults which lead to crack initiation. It is therefore essential to understand this primary damage state in order to model the long term behaviour of the material.

Molecular dynamics (MD) simulation is an excellent tool to probe the displacement cascades produced by a recoil nucleus in various materials (i.e., metals [6,7], ceramics [8–11] and glass [12,13]). The real spatial and time scales covered by such phenomena are on the order of nanometers (nm) and picoseconds (ps) which correspond to the resolution available with the current computers.

Previously, MD displacement cascades were examined on UO_2 by introducing a recoil nucleus of uranium [14,15]. The uranium atom had an initial energy range from 2 to 80 keV. These simulations

* Corresponding author. Tel.: +33 4 66 39 79 40; fax: +33 4 66 79 66 20.
E-mail address: laurent.vanbrutzel@cea.fr (L. Van Brutzel).

0022-3115/$ - see front matter © 2006 Elsevier B.V. All rights reserved.
doi:10.1016/j.jnucmat.2006.07.009

analysed the formation and the spatial distribution of point defects as a function of initial primary knock-on atom (PKA) energy. We showed that high energy projectiles produce several sub-cascades of lower energies in which the main physical mechanisms involved in the production of the primary damage are described.

Herein, several cascades of small energy (5 keV) are used to study the influence of the initial PKA orientation and the temperature on the creation of point defects and point defect clustering. We were also able to examine the primary state damage as a function of dose by studying cascade overlaps.

For this study carried out at 5 keV a box of $32 \times 33 \times 32$ UO_2 unit cells in fluorite structure is created including 393 216 atoms. This size is necessary to contain the full dynamics of the displacement cascade. The system is then relaxed for 5 ps with a constant pressure (0 GPa) and constant temperature (T_{ref}) algorithm. The size of the cubic box depends on T_{ref}. For the three temperatures studied here, the values of the lattice parameter are 0.5469 nm, 0.5472 nm and 0.5475 nm for 0 K, 300 K and 1200 K, respectively. The displacement cascade is initiated by giving an impulsion to a uranium atom in the center of the box in a given direction. This atom will be referred later as the primary knock-on atom (PKA). During the cascade constant volume algorithm with periodic boundary conditions is applied. The temperature of a 0.3 nm wide external layer is kept constant at the temperature T_{ref} by rescaling the velocities to absorb the excess of the kinetic energy which arises from the cascade. A variable time step algorithm is also applied to accelerate the computational time.

The MD calculation was performed using the Born–Mayer–Huggins like empirical potential coupled with a full Ewald summation to describe the coulombic part. The interatomic potential was specifically adapted to reproduce the UO_2 structure, transport properties, and particularly to get realistic energies associated with the formation and migration of local defects. Details of the potential and its validation were reported by Morelon et al. [16].

2. Single cascade

2.1. Influence of the initial direction of the PKA

In order to address the influence of the PKA orientation, 28 cascades of 5 keV have been initiated with different initial directions of the projectile. The PKA was accelerated with four different directions; three in the classical main axis orientations: $\langle 1\,0\,0 \rangle$, $\langle 1\,1\,0 \rangle$ and $\langle 1\,1\,1 \rangle$; and one in the $\langle 2\,1\,0 \rangle$ direction. All the systems were thermalized at 300 K.

Fig. 1 shows the evolution of the number of displaced uranium and oxygen atoms as a function of time and direction of PKA (i.e., (a) $\langle 1\,0\,0 \rangle$, (b) $\langle 1\,1\,0 \rangle$, (c) $\langle 1\,1\,1 \rangle$ and (d) $\langle 2\,1\,0 \rangle$). The error bars in the figures correspond to the standard deviation calculated among the different cascades in a given direction. Here, an atom is considered displaced if it has moved more than 0.1 nm from its initial equilibrium position. The distance of 0.1 nm is chosen such that during the thermal spike only atoms leaving their original lattice positions are taken into account (i.e., atoms vibrating around their current lattice positions are neglected). The evolution of the number of displaced atoms is independent of the direction of the initial PKA (see Fig. 1(a)–(d)). In each of these figures three phases are observed: (i) a ballistic phase that lasts around 0.5 ps where the atoms undergo several collisions and can move over large distances; (ii) a second phase called the thermal spike that lasts for approximatively 0.5 ps where extra kinetic energy brought by the PKA is dissipated via an elastic wave [15]; and (iii) a relaxation phase which corresponds to the recovery of the crystalline lattice [17–19].

At the end of the simulation the number of displaced atoms is approximately the same for all the directions, indicating little or no influence of the initial PKA direction. Overall, the average number of displaced uranium (87) atoms is approximatively 12 times lower than the average number of displaced oxygen atoms (1050). Thus, the oxygen sub-lattice is much more mobile than the uranium sub-lattice.

The influence of the initial PKA direction versus the number of point defects created was also studied. At the end of the simulation the displaced atoms are either located at a crystalline position or at an interstitial site, no antisites were found. Consequently, because the number of atom in the box remains constant, only vacancy-interstitial pairs are created. The association of a vacancy and an interstitial, independently of their spatial separation, is called a Frenkel pair. Fig. 2 depicts the number of Frenkel pairs (N_F) versus the initial PKA direction found at the end of the displacement cascades (10 ps). All the systems were thermalized at 300 K.

The total number of Frenkel pairs created appears to be independent of the initial PKA direc-

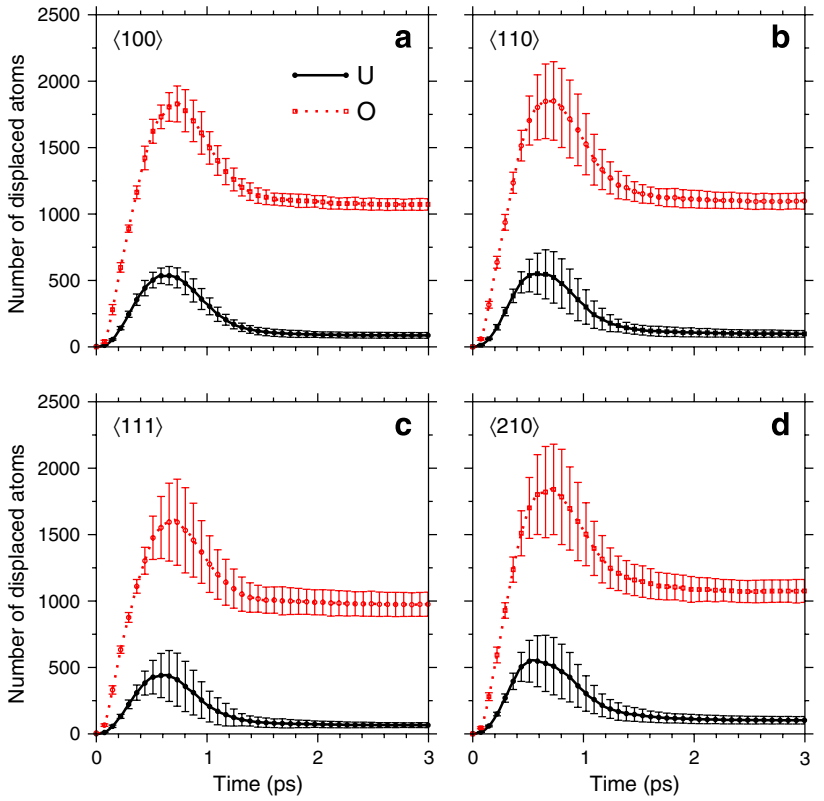

Fig. 1. Number of displaced uranium (solid lines) and oxygen (dotted lines) atoms for four different initial directions of the PKA: ⟨100⟩ (a), ⟨110⟩ (b), ⟨111⟩ (c) and ⟨210⟩ (d). The error bars in the figures correspond to the standard deviation calculated among the different cascades in a given direction.

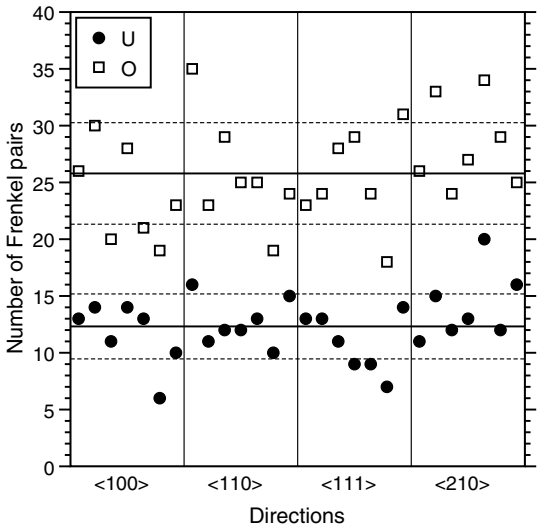

Fig. 2. Number of uranium (●) and oxygen (□) Frenkel pairs for seven simulations per directions (⟨100⟩, ⟨110⟩, ⟨111⟩ and ⟨210⟩). The solid lines represent the mean values and the dotted lines its standard deviations around the mean values.

tion. The number of uranium Frenkel pairs ($N_F(U) = 12.3 \pm 2.8$) created at the end of the cascades is twice smaller than the number of oxygen Frenkel pairs ($N_F(O) = 25.8 \pm 4.7$). These values are rather small considering the total number of displaced atoms at the end of the cascade. Moreover, the ratio of created point defects over the number of displaced atoms at the end of the cascade is substantially different between the uranium and oxygen atoms. 13% of displaced uranium atoms lead to the creation of a stable Frenkel pair while only 2.28% of the displaced oxygen atoms create point defects. This indicates that the oxygen atoms undergo numerous replacements.

Upon examination of the morphologies of the cascades and the distance traveled by the atoms, little dependence is found on the initial PKA orientation. During the course of cascades numerous collisions undergone by the system along with the increase of temperature during the thermal spike render the initial PKA orientation irrelevant. As a consequence, in the following all the results initiated

with different initial directions will be treated as statistically independent cascades.

2.2. Point defects clustering

A cluster is defined when at least two point defects of the same type (i.e., two vacancies or two interstitials) are connected. Point defects are considered to be connected if the distance between two vacancies is in the order of 0.237 nm and the distance between two interstitials is in the order of 0.386 nm. The number of connecting defects defines the cluster size.

Fig. 3 depicts the cluster size distribution averaged over 28 simulations. The interstitial cluster size almost exclusively involves 2–3 point defects, while the vacancy cluster distribution involves clusters up to 18 point defects. Each cascade has one cluster of at least seven vacancies. The fractions of vacancies and interstitials in clusters are equal to 69.5% and 47.9%, respectively. The proportion of clustered interstitials is consistent with the results found in metals where this proportion ranges from 40% to 70% (Fe [21–26], Cu [23,26,27], $NiAl_3$ [27] and FeCu [30]). On the contrary, the proportion of vacancy clusters is significantly higher than in metals (typically 10%). Interstitial clusters in metals are supposed to be thermally stable while vacancy clusters are likely to dissociate at high temperatures which favor recoveries. During the time scale of our molecular dynamic simulations no specific diffusion of the point defects have been observed. Therefore, most of the vacancies which are created during the collision phase in the center of the cascade form rapidly large stable clusters in the core of the cascade.

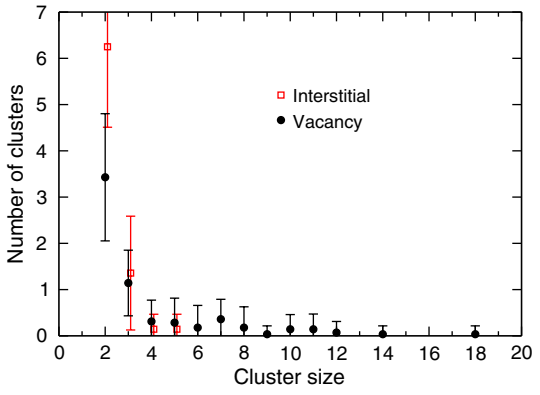

Fig. 3. Vacancies (●) and interstitials (□) cluster size distributions averaged over 28 cascades.

On the other hand, interstitials which are created only at the end of the thermal spike, as observed by Stoller [22], and preferentially at the periphery of the sub-cascade branches form clusters of smaller size. Further simulations, involving diffusion process like kinetic Monte-Carlo need to be carried out in order to study the stability and the spatial evolution of these clusters.

2.3. Temperature influence

Molecular dynamics is commonly used to study the dependence of point defects on temperature. These studies cover a wide variety of materials (Fe [20,22–27], Cu [26], Ni_3Al [27,28] or SiC [29]) and small dependences were found between the variation in temperature and the number of point defects created. This is also true for UO_2. A set of cascades initiated at 5 keV for three different temperatures (0, 300 and 1200 K) has been carried out. The number of point defects created during the cascades is given in Fig. 4. As seen in the figure for both uranium and oxygen atoms, no noticeable differences are found for the various temperatures. This similarities have been observed with simulations which run for over 100 ps. Both interstitials and vacancies are stable at any of the three temperatures at the time scale of the MD simulation. Nevertheless, the

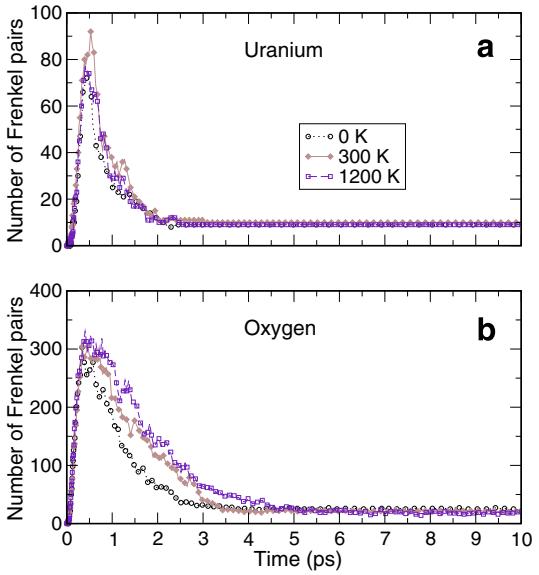

Fig. 4. The number of Frenkel pairs created during displacement cascades initiated at an energy of 5 keV for three different temperatures by chemical species: (a) uranium atoms and (b) oxygen atoms.

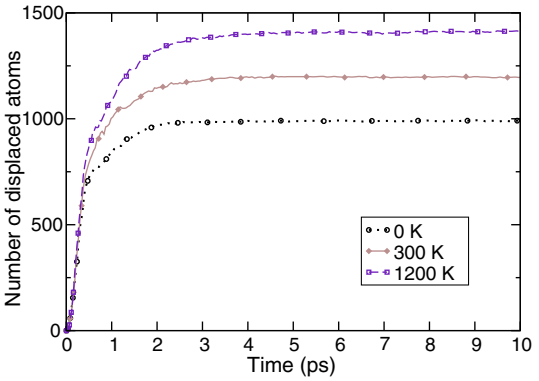

Fig. 5. Evolution of the number of displaced atoms for 3 different temperatures.

number of displaced atoms increases significantly with the increase of temperature (see Fig. 5). This is due to the increase of the atom mobility with temperature.

3. Cascade overlaps

The accumulation of irradiation doses drives the accumulation of point defects in numerous materials. Consequently larger defects appear and can lead to amorphisation and swelling (SiC [31,32]). Although no amorphisation has been observed in UO_2, even for high doses, it is important to comprehend the influence of cascade overlaps in order to study the long-term behaviour. To study this effect, 7 sequences of 11 overlapping cascades initiated at 5 keV and thermalized at 300 K were carried out. Each sequence is construct as follow: An initial cascade initiated with a PKA in the center of the box is run until the end of the relaxation phase (estimated at 6 ps). Consecutively, a second cascade is run, in the same box, with a PKA randomly chosen within a radius of 2 nm from the center of the box with a different initial orientation. This overlapping process is repeated 10 times per sequence. In the following we will denote by c_i with $i = 0, \ldots, 10$ the rank of the overlapping (i.e., C_6 denote the 6th overlaps corresponding to the 7th consecutive cascade).

Usually, in MD simulations of cascade overlaps the MD_{dose} is defined as: $MD_{dose} = N_d \times n_c/N$, where $N_d = 1034$ is the average number of displaced atoms per displacement cascade, n_c is the number of cascades carried out in the simulation box and $N = 393\,216$ is the total number of atoms. The MD_{dose} is measured in MD-dpa. In our simulation the MD_{dose} at the end of the 11th cascade is equal to 2.63×10^{-2} MD-dpa.

3.1. Number of displaced atoms

The evolution of the numbers of uranium and oxygen atoms displaced during the cascade overlap sequence is shown in Fig. 6. No correlation between the heights of the peaks was found. Cascade overlapping does not influence the number of displaced atoms during the ballistic phase. The number of displaced atoms at the end of the relaxation phase increases linearly with the number of cascades. The average number of displaced atoms at the end of the cascades is equal to 110 ± 25 for uranium atoms and 924 ± 138 for oxygen atoms. The behaviour of the two types of atoms is identical, each cascade acts like they were independent. The energy brought by the PKA is dissipated with the same physical process among the cascade overlap sequence.

3.2. Point defects

As already pointed out, the primary damage state is represented by the number of Frenkel pairs (N_F). Fig. 7 exhibits the numbers N_F created during the cascade accumulation sequence. The number of uranium and oxygen Frenkel pairs increases during the first seven cascades. Then it saturates at about 65 uranium Frenkel pairs and 110 oxygen Frenkel pairs. This evolution suggests that an equilibrium exists between the creation and the annihilation of point defects. When the separation distance between a vacancy and an interstitial is small enough, recombination takes place. This recombination is enhanced by the elevated temperature during the successive thermal spikes. This is in agreement with Bacon's studies [23] of spatial cascade overlapping. The number of Frenkel pairs is related to the heat produced during the thermal spike. The creation of point defects is generally related to the evolution of the volumic mass measured in UO_2 matrix under α-decay irradiation. Therefore, this point defect saturation could explain the density saturation phenomenon observed experimentally.

3.3. Point defects clustering

The evolution of the ratio of vacancies and interstitials in a cluster during the overlap sequence is shown in Fig. 8. Both fractions of vacancies and interstitials in a cluster increase significantly with

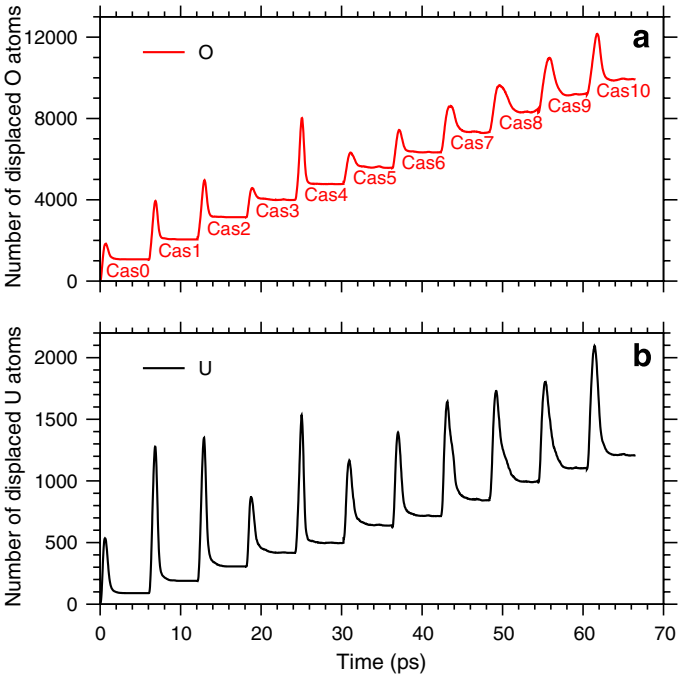

Fig. 6. Numbers of displaced uranium (b) and oxygen (a) atoms during the cascade overlap sequence. Note C followed by a number corresponds to the *i*th consecutive cascade.

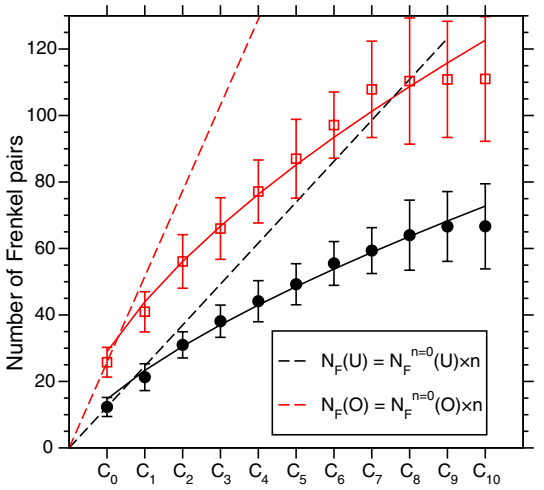

Fig. 7. Numbers of uranium (●) and oxygen (□) Frenkel pairs (N_F) during the cascade overlap sequence. The dotted lines are the linear estimate of N_F defined as $N_F = N_F(0)xn_c$.

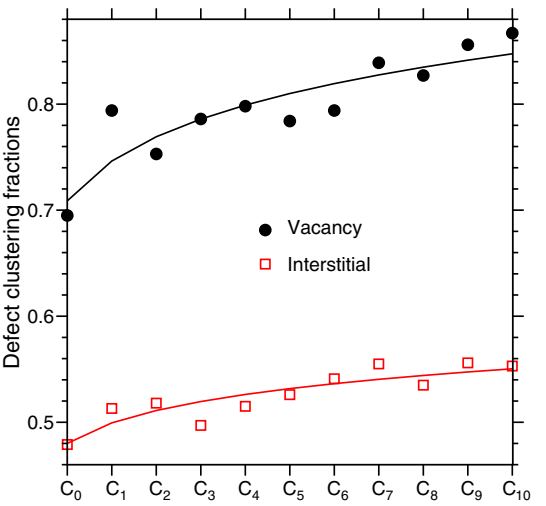

Fig. 8. Fractions of vacancies (●) and interstitials (□) during the overlap sequence.

the MD_{dose}. Nevertheless, as observed previously the evolution of the number of Frenkel pairs saturates for a high number of cascade overlap. This is in agreement with previous studies by Bacon et al. [23] who showed that in SiC two overlapping cascades form less clusters than two independent cascades. As shown in Section 2.2, the fraction of interstitials in a cluster is less than the fraction of vacancies. Cascade overlapping seems to enhance this behaviour.

The increase of the number of defects in a cluster during the overlap sequence is explained by the fact that the new defects are created preferentially near the core of the cascade where some clusters

already exist. Therefore, the probability for these new defects to be attached to a cluster increases. Although, this phenomenon could be applied to both interstitials and vacancies, it is more noticeable for the vacancies because they are preferentially created in the core of the cascades.

More specifically the evolution based on the chemical species increases the fraction of defects in clusters and this is due essentially to oxygen defects. Little difference was found during the first cascade and the eleventh one on the uranium clustering defect. A constant of 85% of the U vacancies and 65% of the U interstitials are in cluster.

The number of small clusters (i.e., size two or three) increases with the MD_{dose}. However, the large clusters increase in size not quantitatively. At the end of the overlap sequence a stable cluster of 54 connected vacancies is created. This cluster could be the precursor to small cavities of 2–3 nm size which play an important role in the precipitation of the gaseous fission products [33].

3.4. Mean displacement

The average distance traveled by an atom from its initial position during the cascade overlap sequence is shown in Fig. 9(a) and (b) for the uranium and the oxygen atoms, respectively. For clarity only the initial (c_0), the fifth (c_5) and the tenth (c_{10}) cascade are displayed. The behaviour at the end of the cascade overlap sequence is identical to the behaviour after the first cascade. All the peaks which correspond to the successive nearest neighbors are in phase. Note that the first peak at 0.2734 nm in Fig. 9(a) corresponds to the distance between a uranium atom and its first interstitial position. The first peak at 0.2734 nm in Fig. 9(b) corresponds to the first oxygen-oxygen distance (d_{O-O}). During the cascade overlap sequence the amplitudes of the three first peaks in Fig. 9(b) decrease and the amplitudes of the following peaks increase slightly indicating that the migration of the oxygen atoms increases. This trend does not appear for the uranium atoms. Nonetheless, more uranium atoms are displaced to their third and fourth nearest neighbor. The oxygen sub-lattice undergoes more collision sequences and is more mobile than the sub-lattice of uranium. Consequently, the reconstruction of the fluorite lattice is relatively fast. Most of the distances traveled by the displaced atoms correspond to the first U–U and O–O nearest neighbours distances which indicated a predominance of the linear collision sequence. On average for 90% of the displaced atoms the distance traveled for both species do not exceed 1 nm at the end of the cascade overlap sequence.

We have also computed the mean-square displacements (MSD) of the displaced atoms during the overlap sequence in order to estimate the a thermal diffusion coefficient. Since the PKA covers a large distance, it is not included in the MSD calculation. The MSD of the atoms at time t is defined by: $\langle r^2 \rangle = \langle |\mathbf{r}_i(t) - \mathbf{r}_i(0)|^2 \rangle$ where $\mathbf{r}_i$ is the position vector of the ith atom. The MSDs reach a plateau at about 5 ps independently of the species and the number of overlap.

Fig. 10 gives the calculated final values of the MSD noted here MSD_∞ for the uranium and oxygen displaced atoms as a function of the MD_{dose}.

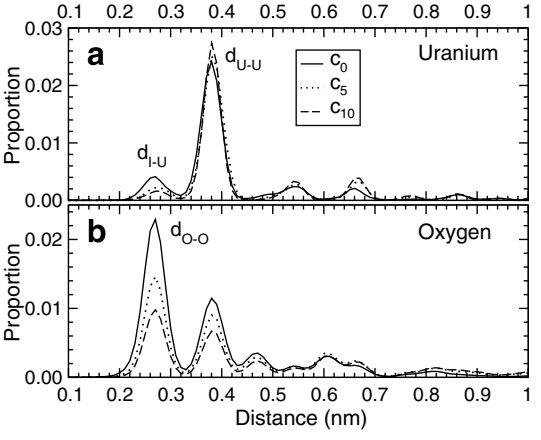

Fig. 9. Distances traveled by (a) uranium and (b) oxygen-displaced atoms during the cascade overlap sequence.

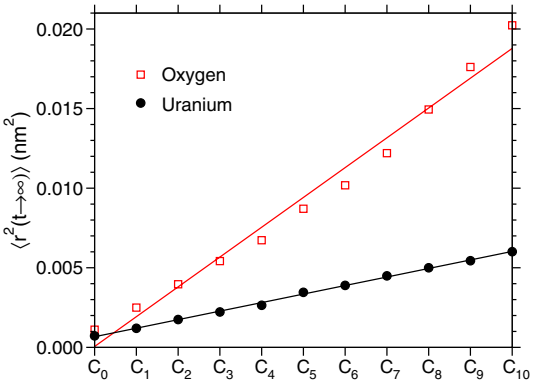

Fig. 10. Evolution of the final value of the mean square displacement for uranium (●) and oxygen (□) as a function of the MD_{dose}.

The MSD_∞ increases linearly with the MD_{dose}. The oxygen MSD_∞ is larger than uranium MSD_∞. This behaviour is consistent with the previous conclusions.

4. Conclusion

This study has shown no influence of the initial orientation of the projectile nor of the temperature on the main feature of the primary damage state, in particular on the number of atoms displaced and on the number of Frenkel pairs created. A large number of vacancies form clusters rather than isolated defects. On the contrary, interstitials are more isolated at the periphery of each branch of the subcascades. This trend is due to their spatial distribution during their creation. Furthermore, the oxygen sub-lattice is more mobile increasing the fraction of oxygen point defects in the clusters. The cascade overlaps show a saturation of the number of point defects created. An equilibrium between the creation of such defects and their recombination is obtained after about seven overlaps. Large stable vacancy clusters of 2–3 nm size is found at the end of the overlap sequence. The analysis of the mean distance traveled and the MSDs of each species shows that the oxygen sub-lattice is affected by the increase in dose since oxygen atoms are more mobile and therefore the vacancies are subject to a greater degree of recombination with interstitials.

Acknowledgment

Calculations have been performed partly at the CCRT at CEA (PC clusters of Alpha machines composed of ES45 quadri-processor nodes).

References

[1] M.T. Robinson, J. Nucl. Mater. 216 (1994) 1.
[2] W.J. Weber, Radiat. Eff. 83 (1984) 145.
[3] H.J. Matzke, J.L. Whitton, J. Phys. 44 (1966) 995.
[4] M. Fayek, P. Burns, G. Yong-Xiang, R.C. Ewing, J. Nucl. Mater. 277 (2000) 204.
[5] J.P. Stout, G.R. Lumpkin, R.C. Ewing, Y. Eyal, Mater. Res. Soc. Proc. 112 (1988) 495.
[6] D.J. Bacon, T. Díaz de la Rubia, J. Nucl. Mater. 216 (1994) 275.
[7] D.J. Bacon, F. Gao, Y.N. Osetsky, Nucl. Instrum. and Meth. B 153 (2000) 87.
[8] R. Devanathan, W.J. Weber, T. Díaz de la Rubia, Nucl. Instrum. and Meth. B 141 (1998) 118.
[9] J.M. Perlado, L. Malerba, A. Sánchez-Rubio, T. Díaz de la Rubia, J. Nucl. Mater. 276 (2000) 235.
[10] F. Gao, W.J. Weber, R. Devanathan, Nucl. Instrum. and Meth. B 180 (2001) 176.
[11] L. Veiller, J.P. Crocombette, D. Ghaleb, J. Nucl. Mater. 152 (2002) 1.
[12] J.M. Delaye, D. Ghaleb, Phys. Rev. B 135 (2000) 201.
[13] A.K. Abbas, J.M. Delaye, D. Ghaleb, G. Calas, J. Non-Cryst. Solids 315 (2003) 187.
[14] L. Van Brutzel, J.M. Delaye, D. Ghaleb, M. Rarivomanantsoa, Philos. Mag. 83 (2003) 4083.
[15] L. Van Brutzel, M. Rarivomanantsoa, D. Ghaleb, J. Nucl. Mater. 354 (2006) 28.
[16] N.D. Morelon, D. Ghaleb, J.M. Delaye, L. Van Brutzel, Philos. Mag. 83 (2003) 1533.
[17] H.L. Heinish, Radiat. Eff. 129 (1994) 113.
[18] M.W. Guinan, J.H. Kinney, J. Nucl. Mater. 103&104 (1981) 1319.
[19] R.S. Averback, D.N. Seidman, Mat. Sci. Forum 15-18 (1987) 963.
[20] A.F. Calder, D.J. Bacon, J. Nucl. Mater. 207 (1993) 22.
[21] F. Gao, D.J. Bacon, A.F. Calder, P.E. Flewitt, T.A. Lewis, J. Nucl. Mater. 203 (1996) 47.
[22] R.E. Stoller, J. Nucl. Mater. 276 (2000) 22.
[23] D. J Bacon, A.F. Calder, F. Gao, J. Nucl. Mater. 251 (1997) 1.
[24] R.E. Stoller, J. Nucl. Mater. 233–237 (1996) 999.
[25] F. Gao, D.J. Bacon, P.E. Flewitt, T.A. Lewis, J. Nucl. Mater. 249 (1997) 77.
[26] W.J. Phythian, R.E. Stoller, A.J. Foreman, A.F. Calder, D.J. Bacon, J. Nucl. Mater. 223 (1995) 245.
[27] D.J. Bacon, A.F. Calder, F. Gao, V.G. Kapinos, S.J. Wooding, Nucl. Instrum. and Meth. B 102 (1995) 37.
[28] F. Gao, D.J. Bacon, Philos. Mag. A 80 (2000) 1453.
[29] L. Malerba, J.M. Perlado, A. Sánchez-Rubio, I. Pastor, L. Colombo, T. Díaz de la Rubia, J. Nucl. Mater. 283–287 (2000) 794.
[30] C.S. Becquart, C. Domain, A. Legris, J.C. Van Duysen, J. Nucl. Mater. 280 (2000) 73.
[31] F. Gao, W.J. Weber, Phys. Rev. B 66 (2002) 024106.
[32] F. Gao, W.J. Weber, J. Mater. Res. 18 (2003) 1877.
[33] C. Sabathier, P. Garcia, internal CEA report SESC/LLCC 06-002, 2006.